The Catalytic Role of the Copper Ligand H172 of Peptidylglycine α-Hydroxylating Monooxygenase (PHM): A Spectroscopic Study of the H172A Mutant†

Shulamit Jaron,‡ Richard E. Mains,§ Betty A. Eipper,§ and Ninian J. Blackburn*,‡

Department of Biochemistry and Molecular Biology, OGI School of Science and Engineering, Oregon Health & Science University, Beaverton, Oregon 97006-8921, and Neuroscience Department, University of Connecticut Health Center, Farmington, Connecticut 06030-3401

Received June 5, 2002; Revised Manuscript Received September 5, 2002

ABSTRACT: The spectroscopic characterization of the H172A mutant of peptidylglycine α-hydroxylating monooxygenase (PHM) was undertaken to determine the importance of this Cu_H ligand in the catalytic mechanism of PHM. Mutation of this histidine reduced the activity of the enzyme over 300-fold with little effect on the structure of the oxidized form. However, the reduced enzyme showed a decrease in the average Cu−N(His) distances from 1.96 Å in wild-type PHM to 1.89 Å in H172A associated with a change in the structure of Cu_H from distorted T-shaped planar in the wild type to 2-coordinate in the mutant. Binding of CO was retained at the Cu_M site (similar to wild type), and peptide substrate binding continued to activate a second site for CO binding. Confirmation of this substrate-induced CO binding site at Cu_H was obtained through the observation that loss of the H172 Cu_H ligand caused a 3 cm^{-1} blue shift in the ν(CO) for this copper carbonyl. Possible mechanistic roles for the H172 ligand are discussed.

Many bioactive neuropeptides are amidated at the C-terminus. The enzyme peptidylglycine α-amidating monooxygenase (PAM,[1] EC 1.14.17.3) carries out this post-translational modification in a two-step reaction corresponding to separate enzymatic activities (*1*, *2*), which are located in separate domains of the bifunctional enzyme PAM, or as separate enzymes (*3*, *4*). The first of these enzyme activities, termed peptidylglycine α-hydroxylating monooxygenase (PHM), is responsible for the hydroxylation of the peptide substrate at the α-carbon of a C-terminal glycine (Scheme 1) in a copper-, ascorbate-, and molecular oxygen-dependent manner (*5*−*9*). The product of this reaction is then converted to the amidated peptide and glyoxylate by the zinc-dependent enzyme peptidyl α-hydroxyglycine α-amidating lyase (PAL) (*10*, *11*).

Recombinant cell lines have made it possible to produce a truncated form of PHM termed PHMcc (*12*). This 35 kDa protein consists solely of the residues necessary for monooxygenase activity, and crystal structures of the oxidized, reduced, and substrate-bound/oxidized forms of PHMcc have been published (*13*−*15*). These three structures are similar, with a root-mean-square deviation of C_α coordinates of ∼0.2 Å and show that the copper centers reside in different

Scheme 1

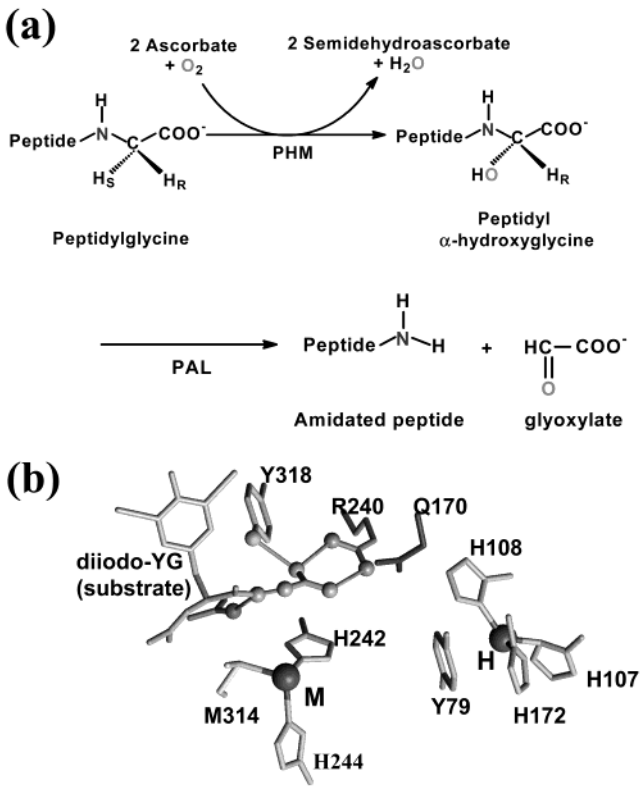

subdomains. The N-terminal subdomain contains Cu_H (the histidine site), coordinated by three histidine ligands: H107, H108, and H172. The C-terminal subdomain contains Cu_M (the methionine site), coordinated by two histidines and a methionine residue: H242, H244, and M314. The two copper centers are separated by an 11 Å solvent-accessible cavity, with no through-bond connecting pathway shorter than 240

† This research was supported by Grants GM27583 (to N.J.B.) and DK32949 (to B.A.E. and R.E.M.) from the National Institutes of Health.

* To whom correspondence should be addressed. Telephone: 503-748-1384. Fax: 503-748-1464. Email: ninian@bmb.ogi.edu.

‡ OGI School of Science and Engineering.

§ University of Connecticut Health Center.

[1] Abbreviations: DW, Debye−Waller; dYVG, dansyl-Tyr-Val-Gly; ET, electron transfer; EXAFS, X-ray absorption fine structure; FT, Fourier transform; HPLC, high-pressure liquid chromatography; IR, infrared; PAL, peptidyl α-hydroxyglycine α-amidating lyase; PAM, peptidylglycine α-amidating monooxygenase; PHM, peptidylglycine α-hydroxylating monooxygenase; XAS, X-ray absorption spectroscopy; YVG, α-*N*-acetyl-Tyr-Val-Gly.

10.1021/bi020404z CCC: $22.00
Published on Web 10/10/2002

Å. The peptide substrate α-*N*-acetyl-diiodo-Tyr-Gly binds in a pocket close to Cu_M, leading to the proposal that dioxygen binds to the Cu_M site as previously suggested for the related enzyme dopamine *β*-monooxygenase on the basis of spectroscopic and kinetic data (*16*, *17*). In this scenario, the second electron required to hydroxylate the C−H bond must be transferred from the distant Cu_H center (*9*, *18*, *19*), which poses intriguing questions relating to the mechanism and pathway of electron transfer.

The only major changes among oxidized, substrate-bound, and reduced forms of PHMcc detected by crystallography were the positions of two residues, Q170 and H108 (a Cu_H ligand). In reduced PHMcc, Q170, and H108 are hydrogen-bonded, whereas in oxidized PHMcc, a water molecule bridges the two residues. Additionally, Q170 is connected to the peptide substrate through a water molecule in the substrate-bound form. Although no crystal structure exists for the reduced substrate-bound form, the combination of data from other forms suggests a possible through-bond connectivity between Cu_H and Cu_M, mediated by the binding of the peptide substrate, which could provide a viable electron-transfer pathway through residues H108, Q170, a water molecule, and the peptide substrate (*14*, *15*).

X-ray absorption spectroscopic (XAS) analysis has led to a different proposal for the electron-transfer mechanism. X-ray absorption fine structure (EXAFS) studies of oxidized and reduced forms of PHMcc indicate that major changes in the coordination spheres surrounding each copper accompany reduction of the enzyme by ascorbate in solution (*20*). The Cu_H center loses its solvating water ligands, and the coordination number is reduced from 4 to 2, with one of the histidine ligands becoming undetectable by EXAFS, implying that it has lengthened by more than 0.3 Å. The Cu_M center also loses coordinated water, with the coordination number dropping to 3. More significantly, the M314 ligand, which is not detected in the EXAFS of the oxidized enzyme, becomes visible at 2.25 Å along with two histidine residues, signaling a movement of the methionine ligand by 0.3−0.5 Å.

Redox-induced changes in conformation and solvation are not characteristic of metal sites designed for rapid electron transfer and are most often seen where the metal center is involved in reactions with exogenous ligands such as dioxygen. Indeed, our previous studies on the wild-type enzyme have demonstrated that both copper sites are reactive toward CO and, by inference, O_2 (*21*). Whereas the wild-type enzyme binds a single CO assigned to a Cu_M−carbonyl with a frequency of 2092 cm^{-1}, binding of peptidylglycine substrates induces a second CO frequency (2062 cm^{-1}) believed to arise from a Cu_H−carbonyl, the CO stretching frequency of which is strongly dependent on the identity of the peptide. Upon the basis of the assumption that binding of CO indicates a potential O_2 binding site at Cu_H, we have proposed a mechanism for electron transfer that differs substantially from the substrate-mediated electron-transfer model (*14*, *15*). In this mechanism, we suggest that dioxygen is first reduced to superoxide at the Cu_H center and that the subsequent electron transfer is mediated by a superoxide molecule, which channels from Cu_H to Cu_M (*21*).

Both mechanisms have interesting and compelling arguments in their favor, and neither can be ruled out at this time. However, if Cu_H is indeed involved in dioxygen binding and reduction, structure/reactivity studies of the Cu_H center and its protein-derived ligands offer a promising approach to distinguishing between the proposed mechanisms. In the present study, we report a detailed structural characterization of the H172A mutant of PHMcc to determine the importance of this Cu_H ligand in catalytic activity. Our results show that mutation of this histidine reduces the activity to less than 1% of that of the wild-type enzyme, with little effect on the oxidized structure. Reduction causes significant structural changes related to a change in the ligand geometry at the Cu_H site. Further, the CO chemistry of H172A provides evidence to support our previous assignment of the peptide-induced CO binding site to Cu_H. These observations have led us to propose possible roles for H172, which include that of an active site base in a modified superoxide channeling mechanism..

MATERIALS AND METHODS

Purification of the Mutant Enzyme. The Chinese hamster ovary cell line expressing the mutant PHMcc protein, H172A, was constructed as described (*12*). Cells were grown in a Cellmax 100 1.1 m^2 hollow-fiber bioreactor (Spectrum) on CSFM as previously described, except that the complete serum-free medium was supplemented with 0.5% Fetal Clone II (Hyclone). Medium containing the expressed enzyme was collected daily, and 7 days worth was combined for each purification. Proteins were purified by column chromatography, which was controlled by a Pharmacia LCC-500 fast protein liquid chromatography (FPLC) instrument. The protocol for protein purification incorporated a two-column process, which resulted in ≥95% pure enzyme. Complete details of cell culture and enzyme isolation were reported previously (*21*).

Calculation of Copper and Protein Concentrations. As isolated, H172A contained <0.3 Cu/protein. Following purification, the protein was dialyzed for 2 days in 0.05 M potassium phosphate, pH 7.5, containing 25 *μ*M Cu^{2+} as $Cu(NO_3)_2$, with a change of buffer after the first day. Following this procedure, the Cu:protein ratio was typically in the range 1.1−1.9. Protein concentrations were determined using the previously determined extinction coefficient for PHMcc (A_{280} = 0.98 for a 1.0 mg/mL solution) (*21*). Copper concentrations were determined by flame atomic absorption on a Varian-Techtron AA5 spectrometer against standard copper solutions spanning the range 5 to 20 *μ*M; all protein samples were diluted to be within this range. In most cases, protein and copper analyses were performed on the same 1 mL sample of enzyme, which eliminated dilution errors from the determination of copper-to-protein ratios.

Specific Activity Measurements. Enzyme activity was determined from the rate of oxygen consumption using a Strathkelvin Instruments 1301 oxygen electrode interfaced with a model 781 oxygen meter, or from the rate of hydroxylation of [^{125}I]-Ac-Tyr-Val-Gly. For the O_2 assay, the reaction mixture consisted of 0.25 *μ*M H172A PHM, 150 mM MES buffer, 13,000 U/ml catalase, 5.0 *μ*M Cu^{2+}, 1.65 mM ascorbate, 0.25 mM peptide substrate, and in some cases various concentrations of imidazole up to 10.5 mM. All reagents except peptide substrate were equilibrated to 37 °C in the cell fitted with the oxygen electrode until a flat baseline was achieved. The reaction was initiated with α-*N*-acetyl-

Tyr-Val-Gly (YVG) and allowed to go to completion. Specific activity, defined as micromoles of O_2 consumed/min/mg of enzyme, was calculated from the initial rate of oxygen consumption. The concentration of oxygen dissolved in air-saturated buffer at 37 °C was taken to be 178 μM, calculated from tabulated data in the Handbook of Physical Chemistry. Wild-type PHM was used as a control for activity measurements in this study and had activities ranging between 15 and 20 micromoles of O_2 consumed/min/mg.

For comparison of specific activities and determination of K_m and V_{max} using [^{125}I]-Ac-Tyr-Val-Gly, purified PHMcc (18.5 mg/mL) and PHMcc H172A (23.5 mg/mL) were first diluted 10-fold into 20 mM sodium TES, 10 mM mannitol, pH 7.0, for analysis by SDS−PAGE. Samples were further diluted for measurement of catalytic activity using assay diluent (20 mM sodium TES, 10 mM mannitol, 1% Triton X-100, 1 mg/mL bovine serum albumin, pH 7.0). Assays were carried out in 75 mM sodium MES, pH 5.5, 0.1 mg/mL catalase (Boehringer Mannheim), 0.5 μM cupric sulfate and 0.5 mM ascorbate, with concentrations of Ac-Tyr-Val-Gly ranging from 1 to 50 μM and approximately 15 000 dpm ^{125}I-labeled Ac-Tyr-Val-Gly. When the same amounts of PHMcc and PHMcc H172A were assayed, PHMcc H172A appeared to be completely inactive. Therefore, to determine whether PHMcc H172A possessed any catalytic activity, an increased amount of mutant protein was assayed. In these experiments, each 40 μL assay tube contained 235 ng of PHMcc H172A or 0.0925 ng of PHMcc.

CO Binding. Binding of CO to H172A PHM was carried out in the following manner. Between 50 and 150 μL of purified H172A (approximately 1 mM) was added to a conical vial fitted with a rubber and silicone septum and kept on ice. In some experiments, Ac-Tyr-Val-Gly was then added to achieve a final concentration of 3 mM. The vial was made anaerobic by gently vacuum flushing with argon no less than eight times with three successive repeats over a period of 40 min. The mutant protein was reduced with a 2-fold excess of ascorbate per copper. Anaerobic conditions ensured the absence of any monooxygenase activity. Carbon monoxide was introduced by vacuum flushing, and the H172A mutant sample was allowed to sit under a CO atmosphere for 20 min. At this time, it was assumed that binding of CO was complete and samples could be removed for infrared and EXAFS analysis.

FT-IR Analysis. Solution IR spectra were recorded on a Perkin-Elmer System 2000 FT-IR with a liquid nitrogen-cooled mercury cadmium telluride detector. Protein solutions were injected into a 0.050 mm path-length transmission IR cell fitted with CaF_2 windows and placed into a constant humidity sample compartment kept at 10 °C. Temperatures below ambient were employed to inhibit the formation of bubbles in the IR sample due to the outgassing of carbon monoxide during data collection. Each sample spectrum consisted of 200 scans, compiled, and background-subtracted using the program Spectrum for Windows (Perkin-Elmer). Subtraction of a water spectrum from the protein spectrum eliminated the large water absorption at 2140 cm^{-1}. This procedure was completed using the interactive polynomial baseline subtraction routine of the Spectrum program.

X-Ray Absorption (XAS) Data Collection and Analysis. XAS data were collected at the Stanford Synchrotron Radiation Laboratory on beam lines 7.3 (BL 7.3) and 9.3 (BL 9.3) operating at 3.0 GeV with beam currents between 100 and 50 mA. An Si220 monochromator with 1.2 mm slits was used to provide monochromatic radiation in the 8.8−10 keV energy range. Harmonic rejection was achieved either by detuning the monochromator 50% at the end of the scan (9731 eV, BL 7.3) or by means of a rhodium-coated mirror with a cutoff of 13 keV placed upstream of the monochromator (BL 9.3). The protein samples were measured as frozen glasses in 20−30% ethylene glycol at 11−14 K in fluorescence mode using either a 13-element (BL 7.3) or 30-element (BL 9.3) Ge detector. To avoid detector saturation, the count rate of each detector channel was kept below 110 kHz, while the rise in fluorescent counts through the edge was kept below 20 kHz per channel. Under these conditions, no dead-time correction was necessary. A Soller slit assembly fitted with a 6 μ Ni filter was used in conjunction with the 30-element detector of BL 9.3 to decrease the elastic scatter peak and further reduce detector saturation. The summed data for each detector channel were then inspected, and only those channels that gave high-quality backgrounds free from glitches, drop outs, or scatter peaks were included in the final average. Data analysis was performed as previously described in detail (*20*, *22*). First, a blank data file collected under identical conditions and detector geometry was subtracted from the summed experimental data. This procedure removed any residual Ni K_β fluorescence which was still present in the detector window, and it produced a flat preedge close to zero. Background subtraction was carried out using the PROCESS module of EXAFSPAK (*39*) using a Gaussian preedge and fourth-order spline fit with k^4 weighting in the postedge region. The E_0 (start of the EXAFS) was chosen as 8985 eV, and the k^3-weighted data were Fourier transformed over the range $k = 2.6-12.8$ Å^{-1}. Simulations (including the calculations of phases and amplitudes) were performed by curve fitting using the program EXCURVE (curved-wave small atom approximation) (*40*) as previously described (*20*, *22*). This allowed for inclusion of multiple scattering pathways between the copper center and (a) the atoms of imidazole rings of histidine residues and (b) the near linear CO coordination. Coordination numbers of protein derived residues were fixed at their crystallographic values. Parameters refined in the fits were distances and Debye−Waller (DW) factors for Cu-ligand interactions. E_f, a small correction to the threshold energy E_0, was also refined but was constrained to take the same value for all shells of scatterers. The amplitude reduction factor was set at 0.90. The goodness of fit was judged by a fitting parameter, F, defined as

$$F^2 = \frac{1}{N}\sum_{i=1}^{n} k^6(\text{Data}_i - \text{Model}_i)^2$$

where N is the number of data points.

RESULTS

Copper Binding Stoichiometry. Table 1 lists the copper binding stoichiometry for a number of individual preparations of H172A. The average copper-to-protein ratio was 1.4:1, which can be compared with values in the range 1.5−2.1, typically found for wild-type PHMcc prepared and measured under identical conditions (*21*). The crystal structure of wild-

Table 1: Copper: Protein Stoichiometry for Independent Preparations of H172A PHMcc

preparation	[Cu] (mM)	[protein] (mM)	Cu:protein
1	3.300	1.700	1.9
2	1.500	0.971	1.5
3	0.403	0.300	1.3
4	0.175	0.179	1.0
5	1.365	1.000	1.4
			average 1.4 ± 0.3

type PHMcc implicates H172 as an important Cu_H ligand, and removal of this ligand would be expected to disrupt copper binding at this site. Interestingly, there appears to be partial or complete retention of copper binding to Cu_H in H172. One explanation is that H172 may be a weak copper ligand in wild-type PHM and may make only a limited contribution to the stability of Cu_H binding. Another possibility is that some other molecule or residue is recruited to substitute for H172 and stabilize copper binding at this site.

Steady-State Activity of H172A and Lack of Rescue by Imidazole. Wild-type PHM consumed 21 ± 3 μM O_2/min/mg with saturating amounts of Ac-Tyr-Val-Gly substrate, while the H172A mutant measured in the same way time had a specific activity of <0.065 μM O_2/min/mg (<0.3%). A similar result was obtained using [^{125}I]-Ac-Tyr-Val-Gly to follow the conversion of Ac-Tyr-Val-Gly into Ac-Tyr-Val-α-hydroxyglycine: the K_m values measured for PHMcc (11.5 μM) and for PHMcc H172A (18.3 μM) were similar, but the V_{max} values differed by a factor of 1000; the mutant had ~0.1% of the wild-type activity. Thus, mutation of H172 causes almost complete loss of PHM activity without significant loss of copper binding at Cu_H, establishing an essential role for H172 in catalysis. An attempt to rescue turnover in H172 by the addition of an excess of imidazole was unsuccessful. Theoretically, if the reactivity of Cu_H toward oxygen were solely reliant upon the coordination of a third histidine ligand, addition of exogenous imidazole would increase the activity of H172 (*23*). However, addition of imidazole had no effect on the rates of oxygen consumption or product formation by the H172A mutant.

FT-IR Spectroscopy of CO Binding to H172A with and without Bound YVG. Binding of the oxygen analogue, CO, to H172 was studied using infrared spectroscopy. Infrared spectra of CO bound H172A in the presence and absence of peptide substrate Ac-Tyr-Val-Gly are shown in Figure 1. In the absence of Ac-Tyr-Val-Gly, H172A binds CO with a stretching frequency of 2092 cm^{-1} (Figure 1a). An identical CO stretching frequency at 2092 cm^{-1} was found in wild-type PHM-CO and half-apo PHM-CO, and this frequency was assigned to a copper−carbonyl at the methionine-ligated copper, Cu_M (*21*, *24*). Assuming that the Cu_M center remains intact in the H172A mutant, the 2092 cm^{-1} CO stretch can also be assigned as a Cu_M−carbonyl.

Addition of Ac-Tyr-Val-Gly activates a second CO binding site in H172A with an IR stretching frequency of 2065 cm^{-1} without loss of CO binding at Cu_M (Figure 1b). A similar result was observed for wild-type PHM where binding of substrate activated a CO binding site with an IR frequency of 2062 cm^{-1} (*21*). Mutation of H172 gives rise to 3 cm^{-1} blue shift of the substrate-activated CO stretching frequency, suggesting that H172 is involved in this CO binding site or at least influences its frequency.

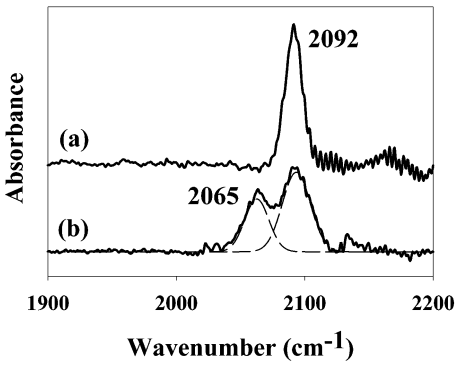

FIGURE 1: Infrared spectra of CO binding to H172A (a) in the absence and (b) presence of the peptide substrate Ac-Tyr-Val-Gly. The doublet in spectrum (b) was fit by a pair of Gaussian peaks with frequency maxima at 2092 and 2065 cm^{-1}, respectively. Spectral intensities are corrected for concentration differences between the protein samples.

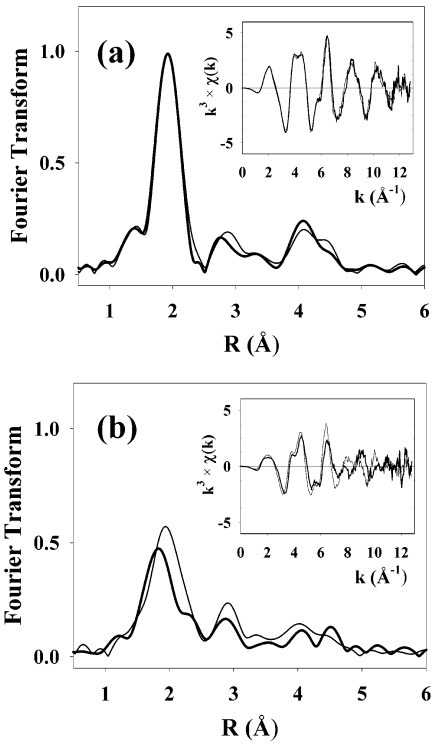

FIGURE 2: Comparison of the Fourier transforms and EXAFS (insets) for the H172A (thick lines) and wild type (thin lines) PHMcc. (a) Oxidized and (b) reduced proteins.

Quantitation of IR bands, and calculation of molar absorptivity from integrated intensities, was complicated by uncertainty in the site occupancy of the copper centers. As shown in Table 1, the H172A mutant has a decreased affinity for copper and exhibits Cu/P binding ratios less than 2. This means that differences in intensity could arise either from differences in molar absorptivity or from differences in site occupancy. For this reason, quantitation of IR bands was not attempted.

X-Ray Absorption Spectroscopy of the Oxidized H172A Mutant. Figure 2 compares Fourier transforms and EXAFS of H172A with those of the wild-type enzyme. For the oxidized enzymes (Figure 2a), the spectra are essentially superimposable, indicating that removal of the H172 imidazole side chain causes no detectable perturbation in EXAFS-sensitive structural elements. Figure 3 shows the

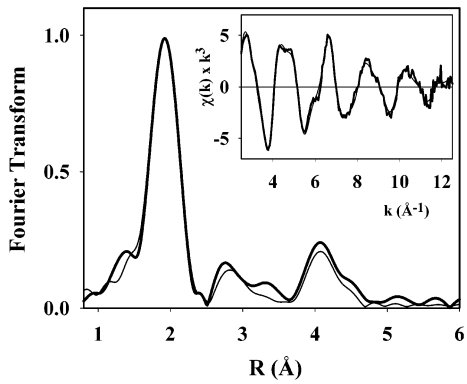

FIGURE 3: Experimental (thick line) versus simulated (thin line) Fourier transform and EXAFS (inset) for oxidized H172A PHMcc. Parameters used to simulate the spectra are given in Table 2.

experimental versus simulated data for oxidized H172A, and Table 2 lists the first shell parameters used to simulate the data of two independent preparations (the fits also include single and multiple scattering contributions from outer shell atoms of histidine-derived imidazole rings at structurally consistent positions). The spectra were fit with an average of four O/N first shell scatterers at a distance of 1.96 ± 0.01 Å. The single, strong absorption in the Fourier transform at 1.96 Å is typical of the histidine/solvent coordination seen in oxidized wild-type PHM (*20*). Simulations, including a first-shell S(Met314), were excluded because they gave no improvement in the fit index, indicating that the Cu−S bond must be weak and/or long in oxidized H172A. The EXAFS spectra provide an averaged structure for all coppers in the protein, and therefore it cannot be determined whether (a) the Cu_H center has been eliminated, leaving a 4-coordinate Cu_M center, or (b) whether the data represent the average of both sites. Since the samples of H172A used for XAS had Cu/protein ratios >1.2, there is more than one copper site, and interpretation (b) is strongly favored. The structure of the oxidized mutant enzyme is indistinguishable from oxidized wild-type PHM via EXAFS, where we used a process termed first shell contour mapping to generate surfaces describing the variation of least-squares fitting parameter *F* with the first shell N and O coordination numbers (*20*). This analysis discriminated in favor of 4-coordination but (as expected) was unable distinguish N(imidazole) from O(water) better than ±1. A similar analysis of the H172A oxidized data (not shown) gave identical results. Therefore, we conclude that, like oxidized wild-type PHM, oxidized H172A has two 4-coordinate copper sites ligated only by histidines and water, suggesting that H172 is replaced by a water molecule in the oxidized derivative.

XAS of Reduced H172A. For H172A, as for wild-type enzyme, dramatic structural changes occur following reduction (compare Figure 2b to Figure 2a). In addition, the FT and EXAFS data of reduced H172A differ significantly from those of the wild-type enzyme (Figure 2b). Figure 4a shows the best fit simulations of the mutant data with first shell fits for three independent preparations listed in Table 2. The simplest analysis treated the spectra as an average of the copper coordination (2 N and 0.5 S), and the first-shell data are fit with 2 N(His) at 1.89 ± 0.01 Å and 0.5 S(Met) at 2.23 ± 0.01 Å (Table 2: S398A, S799A, S200A). For comparison, the reduced wild-type enzyme has the Cu−N shell at 1.96 Å, indicating that the average Cu−N distance is shortened by 0.07 Å in H172A, with either one or both copper sites being affected by the mutation. Because the coppers are separated by 11 Å, it seems unlikely that mutation at the Cu_H site should have a great effect on the Cu_M site.

In the wild-type enzyme, we showed that more meaningful simulations could be achieved by simulating the reduced EXAFS data with a split histidine shell, which allowed the contribution from each copper to be fit separately (*20*). We therefore applied this approach to the H172A data, and the results of the split imidazole shell fits are also listed in Table 2 (S398B, S799B, S200B). The two-site model is seen to fit Cu_H, with two imidazoles at 1.83 ± 0.01 Å, and Cu_M, with two imidazoles at 1.96 ± 0.02 Å and one S(Met) at 2.24 ± 0.02 Å. However, these fits are of comparable quality to those without the split histidine shell (the goodness of fit parameter was within 10% of that with a single shell) and thus do not necessarily establish the validity of the simulation approach since of necessity they increase the number of variable parameters in the fits. Interestingly, copper ligand distances at the Cu_M site are essentially unchanged from those found in the wild type, while Cu−N(His) distances at Cu_H are significantly shorter (1.83 vs 1.88 Å in the wild type) and are at or below Cu−N bond lengths expected for 2-coordinate complexes (*25*).

Like the wild type, reduction of the mutant enzyme with ascorbate appears to shorten the Cu−S(Met) bond, indicated by the appearance of a distinct sulfur EXAFS contribution at 2.24 Å which is unaffected by utilizing the split imidazole model. However, the DW value for the Cu−S bond is high, >0.015 $Å^2$ for a copper site with a single Cu−S bond distance. Large DW terms for this shell have also been observed in reduced wild-type PHM at pH 7.5 (*21*), suggesting the coexistence of different "methionine-on" and "methionine-off" conformations. The CO complex of the H172A mutant exhibits a better-defined Cu−S(Met) shell and a 0.07 Å increase in the Cu−S bond length to 2.31 Å (Figure 4b). In addition, simulations indicate the presence of 0.5 Cu−C(CO) at 1.81 Å and 2 Cu−N(His) at 1.96 Å. These metrical parameters are close to those previously reported for the wild-type enzyme (*21*) and are characteristic of a 4-coordinate Cu_M−carbonyl. Thus, in keeping with the IR data, the CO binding chemistry of H172A appears to be only minimally perturbed in the mutant.

EXAFS data for reduced and carbonylated H172A derivatives were also recorded in the presence of Ac-Tyr-Val-Gly. In all cases, peptide binding caused no change in the spectra (data not shown).

X-Ray Absorption Edges. It is possible to distinguish 2- and 3-coordinate Cu(I) sites by the position and intensity of the edge feature in the X-ray absorption near edge structure (XANES) region of the XAS spectrum. Model compounds of Cu(I) complexes have been used to assign the intense feature at 8983 eV to a 1s → 4p transition and to show that variation in this peak can be correlated with the copper ligand geometry and coordination number (*26*, *27*). The amplitude of this peak was found to be directly dependent on the geometry, with linear 2-coordinate complexes having the highest intensity of the 8983 eV peak. Figure 5a shows the absorption edge data for reduced H172A compared with that of the reduced wild-type enzyme (Figure 5b). The edge

Table 2: EXAFS Fitting Parameters for a Number of Different Preparations of the Oxidized and Reduced H172A Mutant of PHMcc and Derivatives with Bound CO[a]

	N(His)/O(water)			S(Met)			C(CO)			
sample	no	distance	DW	no	distance	DW	no	distance	DW	*F*
				H172A Oxidized						
S799*	2 His	1.96	0.012							0.167
	2 O	1.96	0.012							
S200	2 His	1.96	0.008							0.213
	2 O	1.96	0.013							
				H172A Reduced						
S398A	2 His	1.90	0.013	0.5	2.23	0.020				0.379
S398B	1 His (H)	1.83	0.002	0.5	2.24	0.017				0.380
	1 His (M)	1.95	0.002							
S799* A	2 His	1.89	0.013	0.5	2.23	0.015				0.547
S799* B	1 His (H)	1.83	0.002	0.5	2.25	0.013				0.523
	2 His (M)	1.96	0.002							
S200A	2 His	1.89	0.011	0.5	2.23	0.022				0.376
S200B	1 His (H)	1.83	0.002	0.5	2.23	0.022				0.389
	1 His (M)	1.94	0.002							
				H172A CO						
9799*	2 His	1.97	0.007	0.5	2.31	0.012	0.5	1.81	0.002	0.730

[a] Distances are quoted in Å and DW factors in Å^2. Coordination numbers for histidine and methionine shells were fixed at their crystallographically determined values either averaged over both copper sites (A) or with histidine coordination numbers refined as two separate shells corresponding to each copper center (B). Errors in exogenous ligand coordination numbers (OH_2, CO) are typically ±25%, while errors in distances are ±0.02−0.03 Å (estimated from fits to a number of independent samples). *F* refers to the goodness of fit parameter defined in the text. The fits shown in Figures 3−5 are marked with an asterisk.

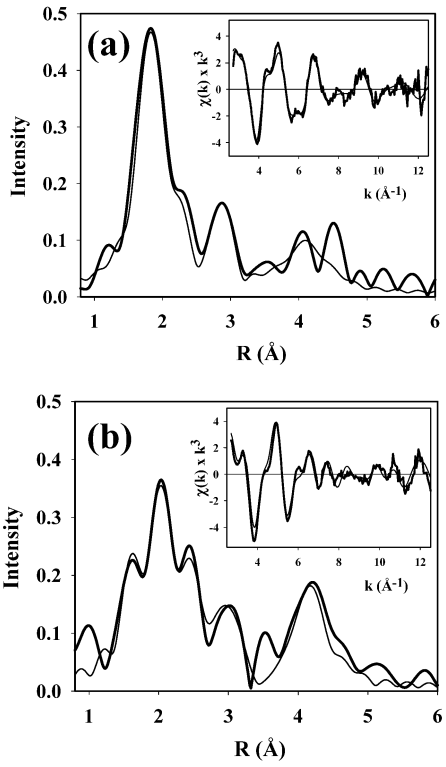

FIGURE 4: Experimental (thick line) vs simulated (thin line) Fourier transforms and EXAFS (inset) for (a) reduced H172A and (b) H172A plus CO. Parameters used to simulate the spectra are given in Table 2.

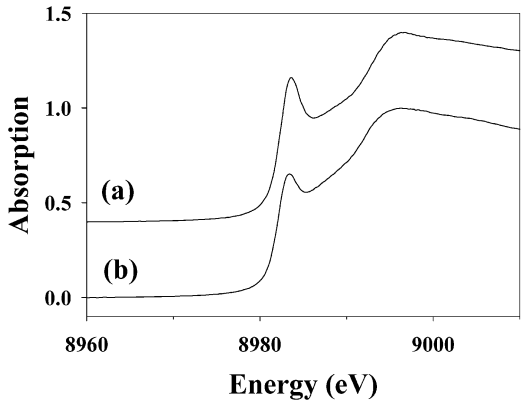

FIGURE 5: X-ray absorption edge data for (a) H172A and (b) wild-type PHMcc. The increased intensity of the 8983 eV edge feature indicates a lower average coordination number in the H172A mutant.

feature of H172A is significantly more intense, suggesting lower coordination for the copper centers in H172A.

DISCUSSION

Structure of the Copper Centers in H172A. The results from copper-to-protein stoichiometry measurements (Table 1) show copper binding ratios between 1.0 and 1.9 for oxidized H172A reconstituted under identical conditions as used previously for the wild-type enzyme. The average of the data falls at the low end of the range of copper binding ratios generally found for the wild-type enzyme and thus suggests that the strength of copper binding is comparable in the H172A mutant. XAS analysis of the oxidized wild-type enzyme previously determined that Cu_H is a 4-coordinate center with H107, H108, H172, and water as ligands (*20*, *28*). Since H172 is a Cu_H ligand in the wild-type oxidized enzyme, the retention of copper binding in the H172A mutant must be the result of recruitment of another ligand, probably a second water molecule, to maintain the preferred 4-coordinate geometry.

EXAFS analysis of the oxidized H172A protein is in agreement with this premise. The data are almost superimposable on those of the wild-type enzyme. The ability of EXAFS to distinguish between O from solvent and N from imidazole is limited to analysis of the outer shell scattering from the C_β and C_γ/N_γ atoms of the imidazole ligand. The precision of such measurements seldom exceeds ±25%, and

replacement of an imidazole by a water ligand at Cu_H is not expected to be detectable by EXAFS. The fit to the oxidized H172A EXAFS data shown in Table 2 utilized two imidazoles and two waters, which is entirely consistent with our conclusion that the site occupied by H172 has been replaced by an O-donating ligand, most probably solvent.

The EXAFS data for the reduced protein are also consistent with the premise that copper remains bound to the histidine site in the reduced enzyme. Previous XAS on wild-type enzyme provided compelling evidence that one of the three histidine residues at Cu_H is only weakly bound in the reduced enzyme (*20*). The data supporting this conclusion were (a) a short 1.88 Å Cu−N bond length for one set of Cu−imidazole distances when the Cu−imidazole shell was allowed to split in the refinement and (b) an intense 8983 eV edge feature characteristic of 2-coordination in the M314I mutant which was shown to contain only the Cu_H site. The analysis of the H172A XAS data shows that removal of H172A enhances this trend and causes the Cu_H site to become rigorously 2-coordinate. This firmly establishes that the weakly bound histidine in wild-type enzyme is indeed H172.

CO Binding to H172A. Carbon monoxide has proven to be a useful molecule for probing oxygen binding to the active sites of PHM. Studies on the wild-type enzyme and a Cu_H-depleted "half-apo" derivative established that in the absence of substrate, CO bound only at the methionine site with a Cu_M−CO frequency of 2092 cm^{-1} (*21*, *24*). However, in the presence of peptide substrate, a second binding site became available for CO, whose frequency was dependent on the nature of the bound substrate. N-Ac-Tyr-Val-Gly induced this second band at 2062 cm^{-1}, while benzoylglycine and benzoylalanine gave bands at 2075 and 2070 cm^{-1}, respectively. We assigned this substrate-dependent band to CO binding at the Cu_H center. In the present study, the substrate-induced CO frequency was found to blue-shift by 3 cm^{-1} to 2065 cm^{-1}. Although small, this shift is highly reproducible and contrasts with the Cu_M−CO frequency at 2092 cm^{-1}, which shows no observable shift in the absence or presence of substrate. We conclude that the 2062 cm^{-1} peptide-induced band in the wild-type protein is therefore influenced by the H172 residue more than the 2092 cm^{-1} band, supporting a Cu_H−CO assignment.

The 3 cm^{-1} shift in the CO frequency of the mutant protein is unusually small if H172 is a ligand to Cu(I) in the Cu_H−CO complex of the wild-type enzyme. A large number of studies on CO complexes of Cu(I) model complexes have established that Cu(I)−carbonyls are overwhelmingly 4-coordinate, with 3-coordination being a rare exception and usually exhibiting CO frequencies in the 2090−2110 range (*29*). Only one example of a 3-coordinate Cu(I)−carbonyl exists with a frequency low enough to be considered a reasonable model for the 2062 cm^{-1} PHM band (*30*). Interestingly, the two ligating N-donors in this complex are sterically constrained by the macrocycle in a fashion similar to the two N-δ coordinating histidines of the contiguous H107 and H108 residues in PHM, where constraints of the β secondary structure also impose steric restrictions on the positions of these residues. Thus, it is possible that the Cu_H carbonyl is a 3-coordinate species similar to the model complex. On the other hand, it is possible that another ligand is recruited to satisfy the tetrahedral preference of Cu(I)−CO adducts. In this scenario, only two candidates appear possible: Y79 and the peptide substrate itself.

Functional Role of H172. What then is the role of the H172 residue in catalysis? Activity is reduced more than 300-fold, but not eliminated, by this mutation. Exogenous imidazole was unable to restore catalytic activity. Imidazole rescued the catalytic activity of heme oxygenase mutants lacking the heme proximal histidine (H25A) (*23*) and restored the spectroscopic signature of the H117G mutant of azurin (*31*). In contrast, imidazole cannot substitute for the proximal histidine of cytochrome *c* peroxidase, rescuing less than 5% of its activity. This suggests that the release of steric restraints imposed by the endogenous proximal histidine eliminates critical interactions between protein, ligand, and metal essential for function (*32*, *33*). The inability of exogenous imidazole to rescue PHM activity in the H172A mutant indicates that the interplay between protein structure and metal coordination is likewise critical.

The essential role of H172 could be due to a number of factors. First, it could poise the redox potential for the Cu_H site at the appropriate value for optimum electron transfer (ET) rates between Cu_H and Cu_M. In the H172A mutant, the data suggest that the oxidized form recruits a solvent molecule to replace the imidazole ligand, while the reduced form is 2-coordinate. The former is expected to decrease the potential, while the latter may increase it due to the increased stability of 2-coordinate Cu(I) systems. Given these two opposing effects, it is not clear how much the potential would be perturbed in H172A. However, the amount of ligand rearrangement accompanying redox would certainly increase (since two solvent molecules are expelled on reduction as opposed to one in the wild-type Cu_H site), thus slowing down the rates of ET. On the other hand, if the only role for H172 is to poise the redox potential of the site, one might expect that imidazole would rescue catalytic activity, at least partially. If the oxidized site easily recruits a water molecule, why not imidazole?

A second possibility is that H172 might provide a steric constraint on the Cu_H site critical for orientating the ET pathway through the neighboring H108 ligand, as suggested in the substrate-mediated ET mechanism, or alternatively via some other ET pathway, such as the Y79 residue which forms a stacking interaction with H172. While this option cannot be ruled out, the weakness of the H172−Cu_H interaction and the facile movement of the residue on reduction suggest significant conformational mobility rather than steric anchoring.

The facile ligand dissociation and rearrangement chemistry demonstrated for the Cu_H center may be more suggestive of substrate reactivity than simple electron transfer. If Cu_H were designed for dioxygen chemistry, then two further possibilities emerge. The first scenario parallels reaction chemistry discovered in the bis dimethylimidazole Cu(I) model system by Sanyal and co-workers (*25*). Here, the 2-coordinate $[(1,2\text{-}Me_2Im)_2Cu(I)]^+$ was found to be unreactive to dioxygen, but addition of exactly one additional equivalent of 1,2-Me_2Im ligand generated a 3-coordinate complex which reacted readily with O_2 at −90 °C to form a meta-stable dioxygen complex. However, whereas binding of the third imidazole in the model system was well-defined by XAS spectroscopy, we have failed to detect any change in structure of either of the copper sites in PHM when substrate binds (*20*). Also,

Scheme 2

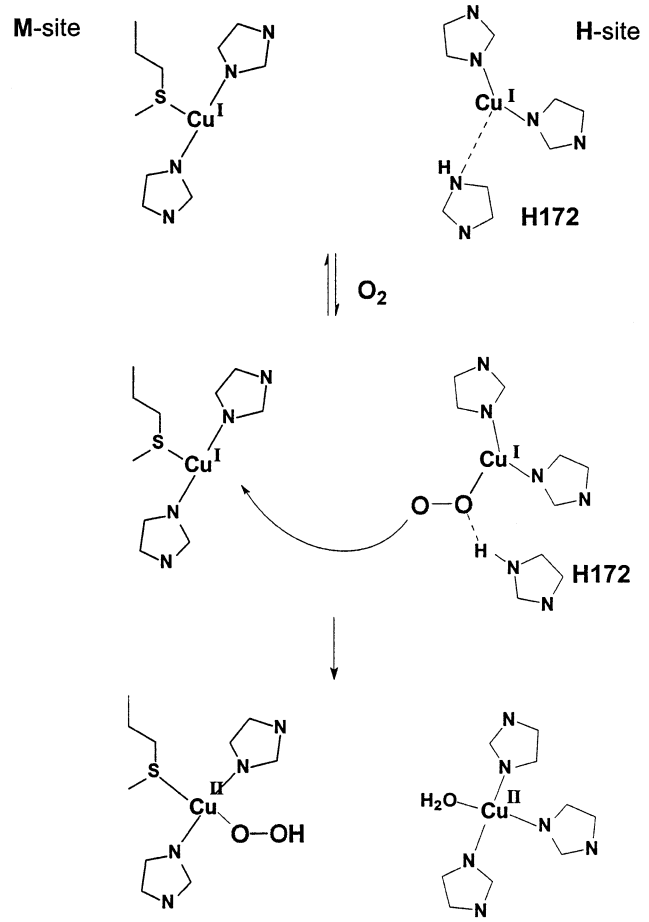

since only the 3-coordinate model precursor is reactive to CO (ν(CO) = 2069 cm^{-1}), binding of CO by the H172A mutant which lacks the third imidazole should be inhibited, contrary to observations.

An alternative hypothesis is that H172 fulfills the role of active site base. The PHMcc catalytic reaction exhibits a pH maximum at 5.5−5.7. This profile suggests the participation of two ionizable groups: one a deprotonated group with pK_a in the range 4−6 and the other a protonated group with pK_a in the range 5−7. With the exception of the coordinated histidine or water ligands, no potential candidates have been identified by the crystal structure. The discovery that H172 is dissociated, and therefore partially protonated at the pH optimum, might suggest a role for this residue in the protonation of the putative Cu(II)−superoxide intermediate formed when dioxygen reacts with Cu_H. Transfer of a proton to the developing superoxide intermediate would leave a deprotonated imidazole ligand ready to coordinate to the copper, thus stabilizing the developing Cu(II) center as required by the preferred 4-coordinate geometry of cupric ion. Interestingly, H172 forms a stacking interaction with Y79 in the crystal structures and thus may be stabilized in the protonated "off" configuration by a cation-π interaction (*34*), as recently suggested for the weakly coordinated histidine residue at the Cu_B center of heme−copper oxidases (*35*−*37*). This mechanism would imply that dioxygen binds to an essentially 2-coordinate Cu_H center, with the protonated H172 residing nearby in an uncoordinated configuration. Interestingly, Tolman and co-workers have recently reported the structure of a Cu(II)−superoxo (or possibly Cu(III)−peroxo) complex formed from the reaction of dioxygen at −80 °C with sterically hindered β-diketiminate Cu(I) complexes containing only two N-donor ligands (*38*, *41*). This chemistry suggests that O_2 can indeed react at Cu_H-like 2-coordinate centers to generate *mononuclear* reduced oxygen intermediates. A modified superoxide channeling mechanism that incorporates this hypothesis is shown in Scheme 2. We note that the proposed reactivity of H172 as an active site base should be observable at some level in the pH dependence of the spectroscopy of the Cu_H site. Such studies are currently underway in our laboratory.

ACKNOWLEDGMENT

We gratefully acknowledge the use of facilities at the Stanford Synchrotron Radiation Laboratory, which is supported by the National Institutes of Health Biomedical Research Technology Program, Division of Research Resources, and by the U.S. Department of Energy, Basic Energy Sciences (BES), and Office of Biological and Environmental Research (OBER).

REFERENCES

1. Young, S. D., and Tamburini, P. P. (1989) *J. Am. Chem. Soc. 111*, 1933−1934.
2. Merkler, D. J., and Young, S. D. (1991) *Arch. Biochem. Biophys. 289*, 192−196.
3. Perkins, S. N., Husten, E. J., and Eipper, B. A. (1990) *Biochem. Biophys. Res. Commun. 171*, 926−932.
4. Kato, I., Yonekura, H., Tajima, M., Yanagi, M., Yamamoto, H., and Okamoto, H. (1990) *Biochem. Biophys. Res. Commun. 172*, 197−203.
5. Merkler, D. J., Kulathila, R., Consalvo, A. P., Young, S. D., and Ash, D. E. (1992) *Biochemistry 31*, 7282−7288.
6. Kulathila, R., Consalvo, A. P., Fitzpatrick, P. F., Freeman, J. C., Snyder, L. M., Villafranca, J. J., and Merkler, D. J. (1994) *Arch. Biochem. Biophys. 311*, 191−195.
7. Tajima, M., Iida, T., Yoshida, S., Komatsu, K., Namba, R., Yanagi, M., Noguchi, M., and Okamoto, H. (1990) *J. Biol. Chem. 265*, 9602−9605.
8. Zabriskie, T. M., Cheng, H., and Vederas, J. C. (1991) *J. Chem. Soc., Chem. Commun.* 571−572.
9. Freeman, J. C., Villafranca, J. J., and Merkler, D. J. (1993) *J. Am. Chem. Soc. 115*, 4923−4924.
10. Eipper, B. A., Perkins, S. N., Husten, E. J., Johnson, R. C., Keutmann, H. T., and Mains, R. E. (1991) *J. Biol. Chem. 266*, 7827−7833.
11. Bell, J., Ash, D. E., Snyder, L. M., Kulathila, R., Blackburn, N. J., and Merkler, D. J. (1997) *Biochemistry 36*, 16239−16246.
12. Kolhekar, A. S., Keutman, H. T., Mains, R. E., Quon, A. S. W., and Eipper, B. A. (1997) *Biochemistry 36*, 10901−10909.
13. Prigge, S. T., Kolhekar, A. S., Eipper, B. A., Mains, R. E., and Amzel, L. M. (1997) *Science 278*, 1300−1305.
14. Prigge, S. T., Kolhekar, A. S., Eipper, B. A., Mains, R. E., and Amzel, L. M. (1999) *Nat. Struct. Biol. 6*, 976−983.
15. Prigge, S. T., Mains, R. E., Eipper, B. A., and Amzel, L. M. (2000) *Cell. Mol. Life Sci. 57*, 1236−1259.
16. Reedy, B. J., and Blackburn, N. J. (1994) *J. Am. Chem. Soc. 116*, 1924−1931.
17. Blackburn, N. J., Pettingill, T. M., Seagraves, K. S., and Shigeta, R. T. (1990) *J. Biol. Chem. 265*, 15383−15386.
18. Brenner, M. C., and Klinman, J. P. (1989) *Biochemistry 28*, 4664−4670.
19. Brenner, M. C., Murray, C. J., and Klinman, J. P. (1989) *Biochemistry 28*, 4656−4664.
20. Blackburn, N. J., Rhames, F. C., Ralle, M., and Jaron, S. (2000) *J. Biol. Inorg. Chem. 5*, 341−353.
21. Jaron, S., and Blackburn, N. J. (1999) *Biochemistry 38*, 15086−15096.
22. Eisses, J. F., Stasser, J. P., Ralle, M., Kaplan, J., and Blackburn, N. J. (2000) *Biochemistry 39*, 7337−7342.

23. Wilks, A., Sun, J., Loehr, T. M., and Ortiz de Montellano, P. R. (1995) *J. Am. Chem. Soc 117*, 2925−2926.
24. Jaron, S., and Blackburn, N. J. (2001) *Biochemistry 40*, 6867−6875.
25. Sanyal, I., Karlin, K. D., Strange, R. W., and Blackburn, N. J. (1993) *J. Am. Chem. Soc. 115*, 11259−11270.
26. Kau, L. S., Spira-Solomon, D., Penner-Hahn, J. E., Hodgson, K. O., and Solomon, E. I. (1987) *J. Am. Chem. Soc. 109*, 6433−6422.
27. Blackburn, N. J., Strange, R. W., Reedijk, J., Volbeda, A., Farooq, A., Karlin, K. D., and Zubieta, J. (1989) *Inorg. Chem. 28*, 1349−1357.
28. Boswell, J. S., Reedy, B. J., Kulathila, R., Merkler, D. J., and Blackburn, N. J. (1996) *Biochemistry 35*, 12241−12250.
29. Pasquali, M., and Floriani, C. (1984) in *Copper Coordination Chemistry, Biochemical and Inorganic Perspectives* (Karlin, K. D., and Zubieta, J., Eds.) pp 311−330, Adenine Press, New York.
30. Villacorta, G. M., and Lippard, S. J. (1987) *Inorg. Chem. 26*, 3672−3676.
31. den Blaauwen, T., Hoitink, C. W. G., Canters, G. W., Ham, J., Loehr, T. M., and Sanders-Loehr, J. (1993) *Biochemistry 32*, 12455−12464.
32. Hirst, J., Wilcox, S. K., Williams, P. A., Blankenship, J., McRee, D. E., and Goodin, D. B. (2001) *Biochemistry 40*, 1265−1273.
33. Hirst, J., Wilcox, S. K., Ai, J., Moenne-Loccoz, P., Loehr, T. M., and Goodin, D. G. (2001) *Biochemistry 40*, 1274−1283.
34. Gallivan, J. P., and Dougherty, D. A. (1999) *Proc. Natl. Acad. Sci. U.S.A. 96*, 9459−9464.
35. Wikstrom, M. (2000) *Biochim. Biophys. Acta 1458*, 188−198.
36. Osbourne, J. P., Cosper, N. J., Stälhandske, C. M. V., Scott, R. A., Alben, J. O., and Gennis, R. B. (1999) *Biochemisty 38*, 4526−4532.
37. Ralle, M., Verkovskaya, M. L., Morgan, J. E., Verkovsky, M. I., Wikstrom, M., and Blackburn, N. J. (1999) *Biochemistry 38*, 7185−7194.
38. Spencer, D. J. E., Aboelella, N. W., Reynolds, A. M., Holland, P. L., and Tolman, W. B. (2002) *J. Am. Chem. Soc. 124*, 2108−2109.
39. George, G. N. (1995), EXAFSPAK Program, Stanford Synchrotron Radiation Laboratory, Menlo Park, CA.
40. Binsted, N., Gurman, S. J., and Campbell, J. W. (1998) EXCURV98 Program, Daresbury Laboratory, Warrington, U.K.
41. Aboelella, N. W., Lewis, E. A., Reynolds, A. M., Brennessel, W. W., Cramer, C. J. and Tolman, W. B. (2002) *J. Am. Chem. Soc. 124*, 10660−10661.

BI020404Z